SSC21-SI-41

Development and Testing of a Low Flame Temperature, Peroxide-Alcohol-Based Monopropellant Thruster

Darren King, Curtis Woodruff, Justin Camp, David Carroll
CU Aerospace, LLC
3001 Newmark Drive, Champaign, IL 61822; 217-390-6498
king@cuaerospace.com

ABSTRACT

Recent developments in chemical propulsion for CubeSats have been directed away from high flame temperature propellants such as the ionic salts and towards cooler propellants that mitigate thermal management issues. Engineers at CU Aerospace have continued the development of a Monopropellant Propulsion Unit for CubeSats (MPUC), which burns a diluted mixture of hydrogen peroxide and alcohol called CUA MonoPropellant #10 (CMP-X). The propellant was subjected to UN classification tests and has been certified for air transport, demonstrating "little to no reactivity as an explosive in the UN Test Series 1 & 2 tests." Recent experimental measurements demonstrate that MPUC with CMP-X operates at a flame temperature below 1000 °C, enabling its manufacture from standard stainless steels and avoiding more costly refractory metal components common with HAN- or ADN-based thrusters. Using hardware optimized for ~150 mN operation, a high-Isp test measured 180 s at 174 mN and a high-thrust test measured 450 mN at 154 s. A preliminary 1.5U design provides 1600 N-s total impulse.

INTRODUCTION

The high toxicity of hydrazine has steered developers towards low-toxicity "green" chemical monopropellants. Considerable advancement and successful flight demonstrations have been made with AF-M315E (now denoted "ASCENT")[1,2,3,4,5,6] and LMP-103S.[7,8,9,10] These monopropellants provide a better product of density x specific impulse than hydrazine with the only principal issues being cost/availability, transportation restrictions, and high catalyst bed / flame temperatures which can create materials and thermal soakback concerns for a spacecraft. CU Aerospace (CUA) began development of a hydrogen peroxide / ethanol monopropellant blend in 2016 that trades 15-20% of those systems' specific impulse performance in order to favorably address these issues.[11] More recently, researchers at NASA Glenn Research Center have also investigated hydrogen peroxide / ethanol blends similar to those previously tested by CUA.[12] While many customers will be primarily driven by highest performance, this propellant and its associated Monopropellant Propulsion Unit for Cubesats (MPUC) anticipates a niche market of customers who are more sensitive to range safety concerns, cost, and other factors.

CUA monopropellant, "CMP" is a stoichiometric mixture of hydrogen peroxide and pure ethyl alcohol. An earlier variant, CMP-8, was formulated to use the highest common concentration of commercially available stabilized hydrogen peroxide (50 % w/w) in order to be as performance-competitive as possible with the SOA green monopropellants for small satellite applications. The reaction is shown in **Eq. 1**, wherein the propellant is combusted over a catalyst. However, CMP-8 contains more than 40% total hydrogen peroxide (~45% by mass), which is not permitted for air transport by the commercial carriers like UPS or FedEx because its H2O2 concentration exceeds 40%.

$$6\ H_2O_2\ (aq) + 1\ C_2H_6O\ (liq) + 11.28\ H_2O\ (liq) = \quad (1)$$

$$2\ CO_2(g) + (9 + 11.28)\ H_2O\ (g) + 2.34\ kJ/g$$

SAFETY AND HANDLING

Hawkins succinctly described desirable monopropellant safety characteristics in 2010, **Table 1**.[13] Detonation tests were carried out on CMP previously, confirming the ternary plots of Shanley, et al., **Figure 1**.[14] The detonation testing performed by CUA, with the assistance of the University of Illinois' Energetic Materials Laboratory, aligns with literature [Shanley, 1958], indicating that CMP-8 is not detonable by blasting cap, electro-static discharge (ESD), or impact. Further dilution from CMP-8 (44.9% H2O2) to CMP-X (39.9% H2O2) increases the overall safety of the solution. CMP-X was recently subjected to UN Test Series 1, 2, 3, and 6. The testing facility, Safety Consulting Engineers / Dekra Process Safety of Schaumburg, IL, recommended that "CMP-X liquid propellant be excluded from the explosives Class". This

rating permits far simpler logistics than those carried by ASCENT (UN Class 1.4C) or LMP-103s (UN Class 1.4S). Long-term storage testing indicates indiscernible fuel degradation in excess of one year in sealed containers.

Table 1 - Desirable monopropellant safety properties [Hawkins, 2010]

Characteristic	Objective
Thermal Stability	<2% by wt. decomposition for 48 hrs at 75 °C
Unconfined ignition response	No explosive response
Impact sensitivity [Olin Mathiesen drop weight]	>20 kg-cm minimum
Friction sensitivity [Julius Peters sliding friction]	Insensitive at high load (≥300N)
Detonability [NOL card gap]	Class 1.3; (Zero-card)
Adiabatic compression [U-tube test]	Insensitive (Pressure ratio of 35)
Electrostatic discharge sensitivity	Insensitive to static spark discharge (1J)
Vapor toxicity	Low hazard (No SCBA requirement)

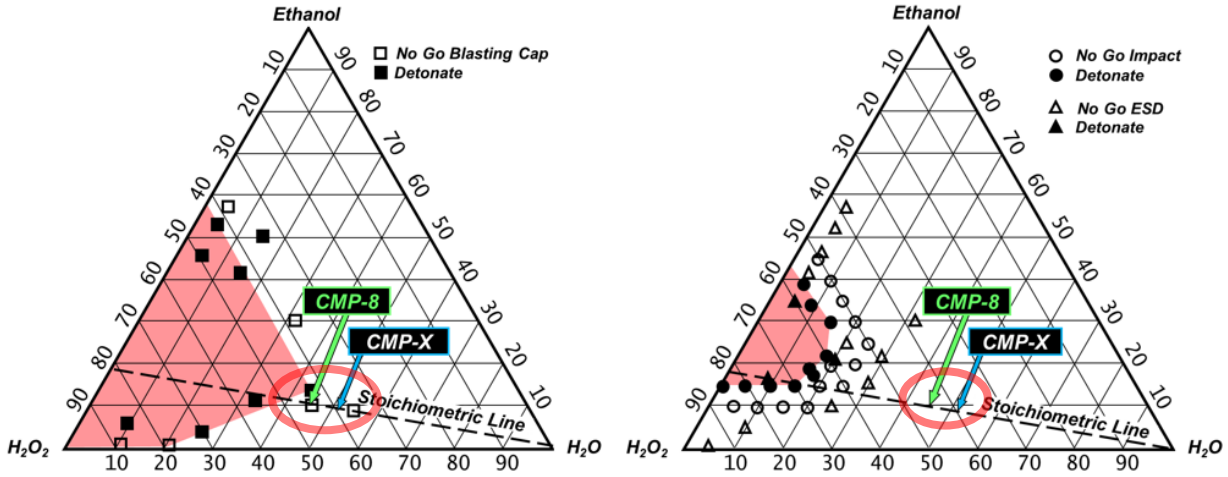

Figure 1. Ternary detonability plots of H_2O_2 / ethanol (blasting cap on left, ESD and impact on right)

The vapor toxicity of CMP is comparable with the other green monopropellants. Vapor pressure was calculated and verified experimentally for CMP-8. The same calculation is used for the diluted CMP-X formulation. On a component level for CMP, H2O2 has the most harmful vapors, and its partial pressure is estimated using Raoult's law and presented in **Table 2**.

Table 2. Characteristics of CMP-X.

Transport Hazard Classification	Excluded from explosives Class 1
Total Vapor Pressure [psia, 20°C]	0.34
Partial Pressure of Hazardous Vapor [psia, 20°C]	0.027 (H_2O_2)
Vapor Toxicity - TLV / TWA [ppm] (threshold limit value / time weighted average)	1 (H_2O_2)
Oral Toxicity - LD_{50} [mg/kg] (median lethal dose)	1000
PPE Required	Spill protection - gloves / goggles
Fuel Availability	>2M Metric tons COTS reagents produced annually
Price per kg [USD]	~$100
Thruster head materials	Non-refractory alloys
Catalyst	Ir–Al_2O_3 or MnO_2
Kinematic Viscosity [cSt, 20°C]	1.4
Minimum Operating Temperature [°C]	< -33
Typical Operational Mode	Continuous
Initial Operational Pressure [psia]	40 - 170
Max Run Time [s]	$m_{propellant}$ / $\dot{m}$
Flame temperature [°C]	900
Pre-Heat Temperature [°C]	220
Vacuum I_{sp}, measured (CMP-X) [s]	180
Propellant Density [g/cc]	1.12
*Density Impulse (I_sd), [g*s/cc, ρ x I_{sp}]*	201
Volumetric Impulse, [N-s/liter]	> 1,100 †

† Anticipated MPUC design with 1300 cc of CMP-X in 2U package with specific impulse ~ 180 s.

By its very nature, the propellant's dilution results in an intrinsically safe material – the thruster is "burning water". Until it is mixed with catalyst, CMP-X combusts no more vigorously than water-diluted ethanol. **Figure 2** shows a test series of ignition attempts demonstrating no ignition unless the CMP-X monopropellant is mixed with catalyst and a heat source.

Figure 2. Photographs showing inherent safety of CMP-X / catalyst system.

MPUC SYSTEM OVERVIEW

The CUA MPUC comprises a pressurant-fed propellant, valved through a decoupling orifice and injected into a screen-retained granular catalyst bed. Bed compression is maintained by a pair of showerhead injector plates, a hard shoulder, and a torqued hex jam nut. From here, the combustion gases enter the nozzle, where they are accelerated and exhausted, **Figure 3**. Various resistive heating solutions have been implemented to date, including nichrome wire, cartridge heaters, and most recently a band heater. The bulk of testing to date has been performed in Combustion Test Fixture (CTF) version "O3" (**Figure 4**). This CTF features rapid reconfigurability with threaded inlet and exit fittings. Earlier variants used a glow plug for ignition assist, but this plug has since been removed and its port left unmachined to help minimize leaks.

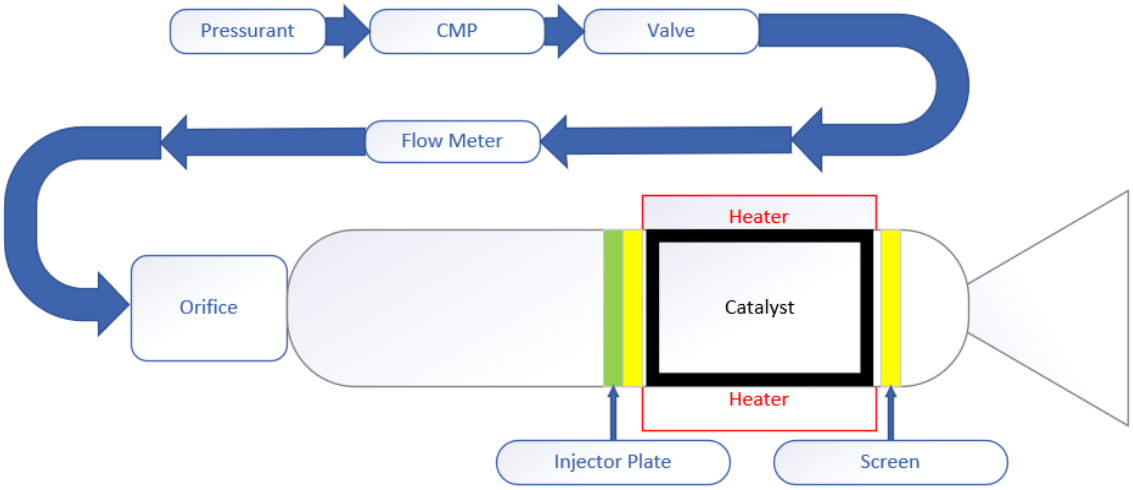

Figure 3. MPUC system diagram.

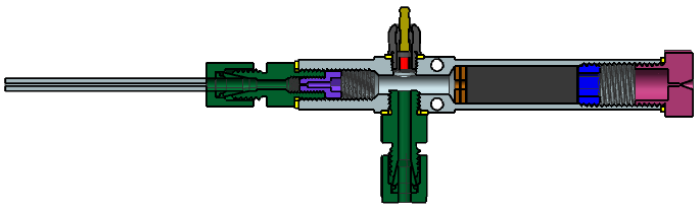

Figure 4. CTF O-3B (flow is left to right)

Early development efforts used granular manganese dioxide. Although plentiful, inexpensive, and robust during low-performance tests, this catalyst demonstrated poor life once internal temperatures of the thruster approached their stoichiometric limits. Accordingly, an in-house version of Shell's widely implemented 405 catalyst was created and used for further testing. Iridium was loaded onto a granular white alumina substrate and the resulting catalyst grains were sifted for size uniformity before loading into CTFs for further testing.

Sealing the inlet and exit fittings is accomplished by copper crush washers between the Series 316 stainless steel body and fittings. Over time, wear on these threads and surfaces became pronounced and a move to a copper-free seal solution was made. The nozzle feature was integrated into the main body in CTF-S, and eventually the inlet fitting was removed in favor of a simple and robust compression fitting connection, **Figure 5**. During bench testing, a five-element thermocouple rake is placed onto the CTF to obtain axial temperature profiles during testing. Note that the CTF-S fixture uses an unoptimized easy-to-manufacture nozzle for testing purposes.

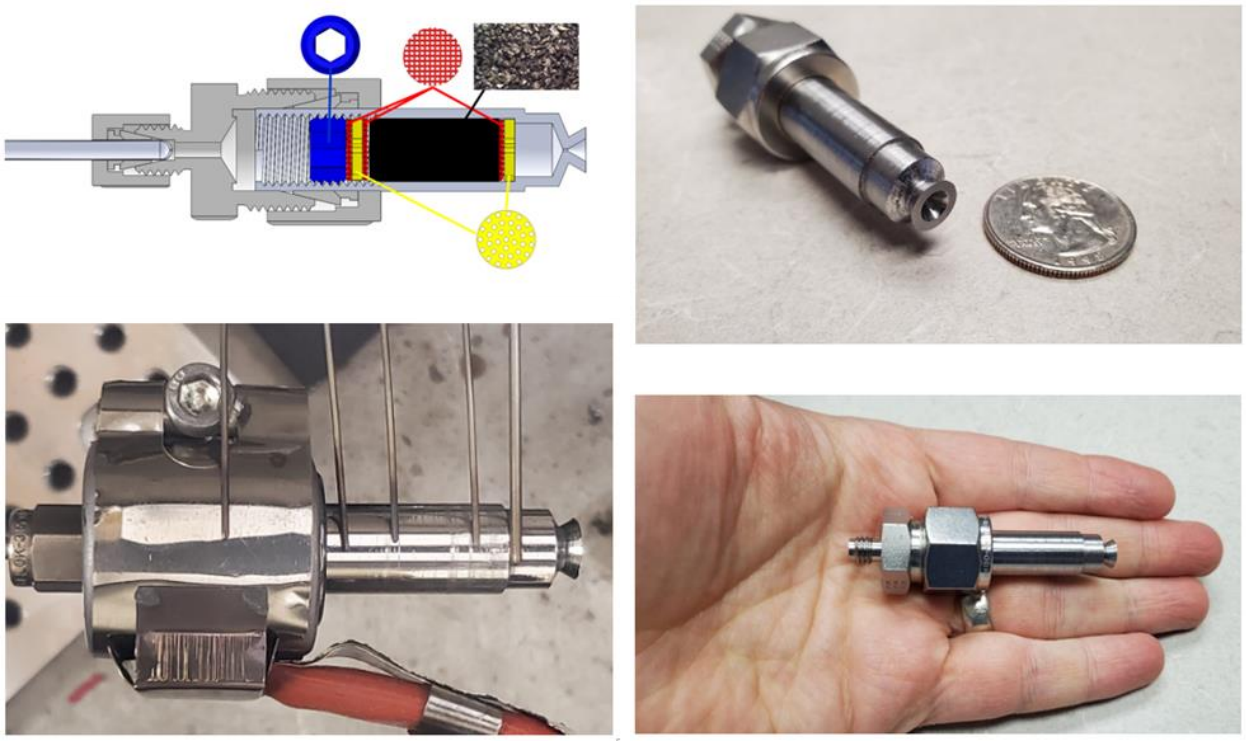

Figure 5. CTF-S (from upper left, clockwise - cross section of the thruster with inlet fitting, blue jam nut, red retention screens, and yellow injector plates; photos of the assembled thruster with items for scale; and the thruster ready for testing with the five-element thermocouple rake in place).

NOZZLE MODELING WITH BLAZE MULTIPHYSICS

To provide a more detailed understanding of the performance of the MPUC nozzle and aid in design to minimize the impact of the boundary layer and maximize nozzle efficiency, CUA utilized its internally developed BLAZE Multiphysics™ Simulation Suite <http://www.blazemultiphysics.com> in order to construct high-fidelity simulations of the MPUC micro-nozzle.[15] BLAZE is comprised of a number of inter-operable and highly scalable parallel finite-volume models for the analysis of complex physical systems dependent upon laminar and turbulent fluid-dynamic (incompressible and compressible subsonic through hypersonic regimes), non-equilibrium gas- and plasma-dynamic, electrodynamic, thermal, and optical physics (radiation transport and wave optics) using any modern computational platform (Windows, Mac, Unix/Linux). BLAZE is compatible with a number of free, open-source, yet commercial quality grid generation and post-processing software packages which greatly reduces training and operating costs. BLAZE is also compatible with state-of-the-art commercial grid generation and post-processing solutions.

BLAZE has been previously applied to simulations of the CUA Cubesat High Impulse Propulsion System (CHIPS) and Monofilament Vaporization Propulsion (MVP) nozzles, as well as to MPUC nozzles during the Phase I effort.[16,17] The gas flows were modeled using the BLAZE Pressure-Based Coupled Navier Stokes and Material Properties models where heat capacity, enthalpy, specific gas constant, gamma, thermal conductivity, and molecular dynamic viscosity were modeled as a function of gas temperature using user input fits in the Material Properties model. All scalar fluxes were modeled using 2nd order schemes with a Barth-Jespersen flux gradient limiter applied only to the second order upwind flux scheme applied to axial momentum flux in order to limit non-physical extrema at FVM cell boundaries. A grid study, not shown for brevity, was performed in order to determine the rectilinear grid density required to limit discretation errors in calculated thrusts to less than 1%. The mass error was converged to < 0.3% of the input mass flow for the simulations presented herein.

During earlier programs, the BLAZE model was validated for MPUC for both CMP-8 and CMP-X data and 2D-axisymmetric grids were constructed to investigate different MPUC micronozzles. In all cases, the geometry modeled had a 0.03556 mm (0.014") diameter throat and a flow rate of 87 mg/s of combusted CMP-X. A flame temperature of 1223 K was assumed. For simplicity, thermal expansion of the nozzle was ignored in these simulations.

The goal of this study is to numerically examine if there are any significant benefits to using contoured micronozzles over straight conical designs (in consideration of potential cost savings for fabrication and polishing of contoured nozzles). One of the obvious contoured nozzle choices to examine is that of the classic Minimum Length Nozzle (MLN) designs computed using a method of characteristics approach. **Figure 6** illustrates the nozzle shape using 20 characteristics resulting in 21 grid points along the contour. **Figure 7** illustrates the corresponding grid that was generated using the 21 grid points as the defining surface. More grid points are included in the BLAZE grid mesh and their locations are determined from a cubic spline fit. Overall, the MLN mesh is 56 cells across the nozzle and 780 cells in the flow direction (231 upstream, 11 in the converging section, 17 in the throat, and 521 downstream of the throat in the MLN portion) for a total cell count of 43,680 cells. Smoothed throat nozzles (rather than sharp-edged) were also investigated with the same number of grid cells.

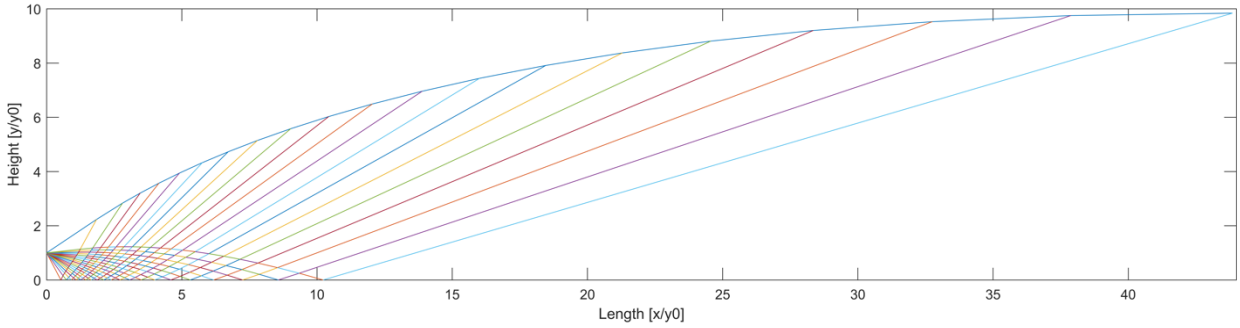

Figure 6. Minimum Length Nozzle (MLN) with 20 characteristics generated using free MATLAB tool. Note that the axes are normalized to the throat height of the nozzle.

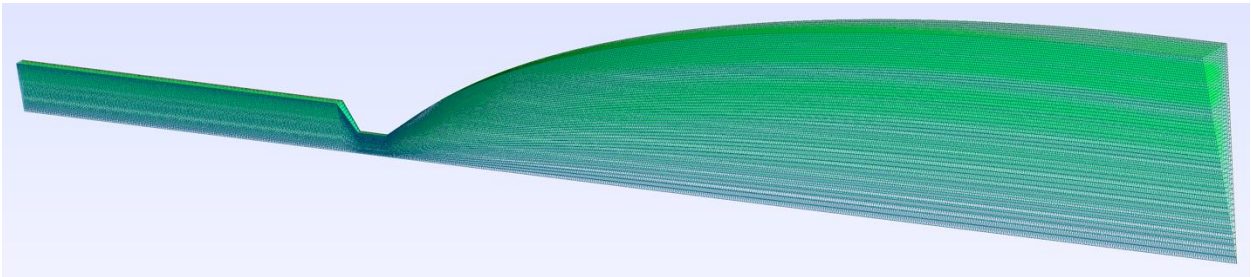

Figure 7. Grid mesh containing 43,680 cells generated for MLN including a plenum and throat section showing the π/16 axisymmetric slice view. Note that the grid density is tighter near the walls to model the nozzle boundary layer more accurately.

Figure 8 (velocity) and **Figure 9** (temperature) illustrate the predicted flow from 2D-axisymmetric BLAZE simulations. Three conical nozzles are shown with area ratios ranging from 51 to 100, all with a 20° divergence half-angle. Also shown are three contoured MLN designs computed using a method of characteristics approach. The MLN with area ratio of 97 is a classic design with a linear sonic line and another approach with a Curved Sonic Line (CSL) was also investigated. The MLN and MLN-CSL cases indicated that the highest flow velocities (and corresponding lowest flow temperatures) were occurring inside the nozzle, so a truncated MLN was also simulated. The smoothed throat cases (both conical and de Laval-type) showed similar characteristics to their counterpart cases.

Case	Area Ratio	Velocity	Velocity Scale
Conical (20°)	51	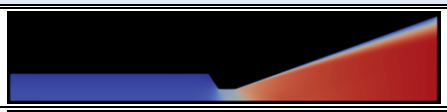	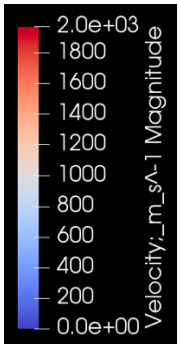
Conical (20°)	70	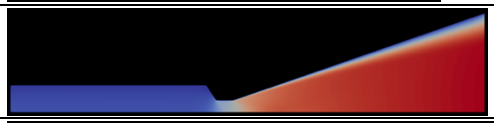	
Conical (20°)	100	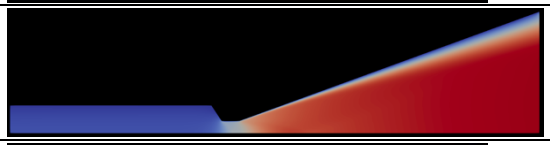	
MLN, truncated	70	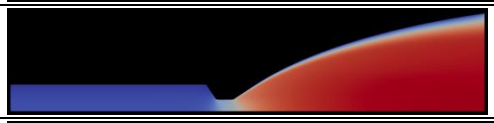	
MLN	97	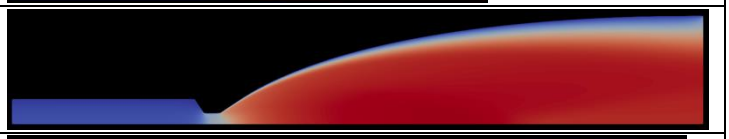	
MLN-CSL	100	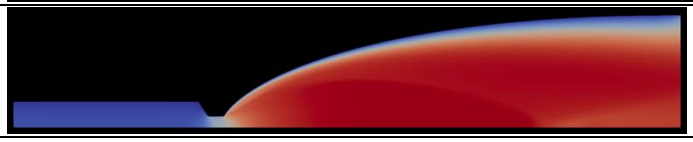	
Conical (20°) w/ smoothed (polished) throat	70	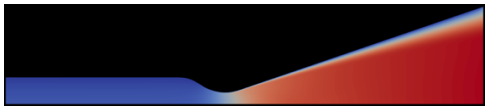	
de Laval nozzle w/ truncated MLN	70	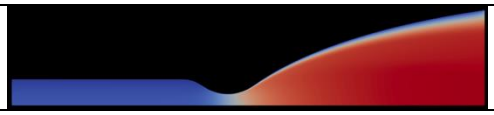	

Figure 8. BLAZE predictions of flow velocity for different nozzles (conical and contoured) with different area ratios. Note that the throat size is kept a constant 0.03556 mm (0.014") in all cases. Illustrated is a 2D half-slice through an axisymmetric nozzle.

Figures 8 and **9** show that the boundary layer for the conical nozzles is minimal and on the order of 10-15% of the nozzle size. The growth of the boundary layer in the extended MLN and MLN-CSL nozzles is larger than for the conical designs and manifests itself as a slight reduction to thrust and Isp, **Table 3**.

A summary of the predicted performance of each of these different nozzles is provided in **Table 5**. It is clear that all of the nozzles perform similarly (the best case is only 4% higher than the worst) and that the best options predicted are the straight conical nozzles with an area ratio of 70 or higher. While the MLN-CSL is slightly shorter in length than the classic MLN, its performance was predicted to be the worst of all the nozzles studied. The smoothed throat cases (both conical and a de Laval-type) showed similar characteristics to their area ratio 70 counterpart cases. Additionally, the MLN contoured nozzles are significantly longer (unless truncated) than the conical nozzles and therefore less desirable for the purposes of miniaturized propulsion systems for CubeSats.

Case	Area Ratio	Temperature	Temp. Scale
Conical (20°)	51	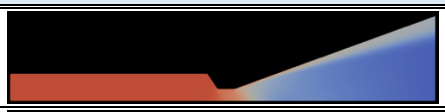	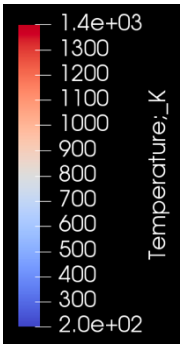
Conical (20°)	70	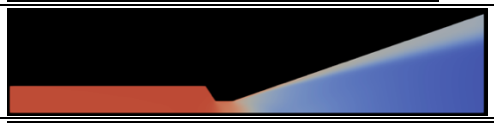	
Conical (20°)	100	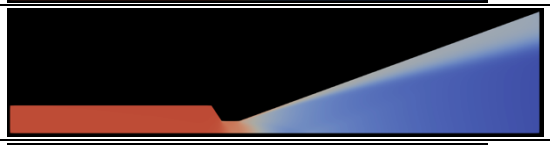	
MLN, truncated	70	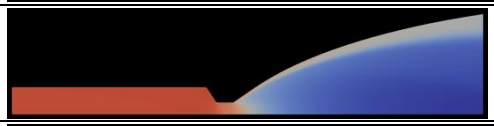	
MLN	97	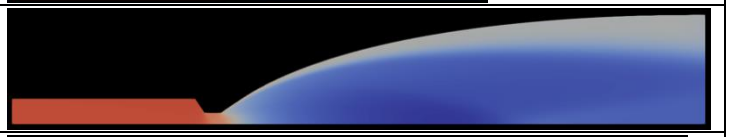	
MLN-CSL	100	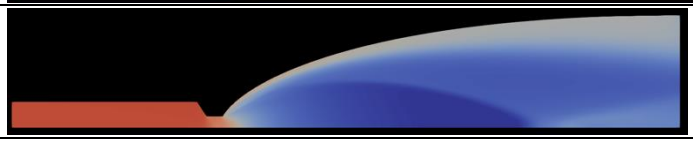	
Conical (20°) w/ smoothed (polished) throat	70	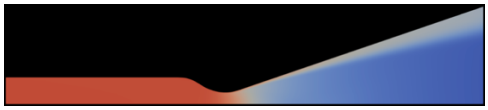	
de Laval nozzle w/ truncated MLN	70	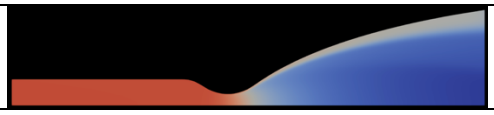	

Figure 9. BLAZE predictions of flow temperature for different nozzles (conical and contoured) with different area ratios. Note that the throat size is kept a constant 0.03556 mm (0.014") in all cases with an inlet temperature of 1223 K. Illustrated is a 2D half-slice through an axisymmetric nozzle.

Table 3. Summary of BLAZE simulations for different nozzles (conical and contoured) with different area ratios. Note that the throat size is kept a constant 0.014" in all cases.

Case	Half-angle (°)	Area Ratio	Div. Noz. Length (cm)	Thrust (mN)	Isp (s)
Conical	20	51	0.295	155.6	182.6
Conical	20	70	0.378	158.0	185.4
Conical	**20**	**100**	**0.435**	**159.4**	**187.0**
MLN	Contoured	70	0.378	157.2	184.4
MLN	Contoured	97	0.775	156.7	183.9
MLN-CSL	Contoured	100	0.725	153.3	179.8
Conical (smooth throat)	20	70	0.392	157.6	184.9
de Laval	Contoured	70	0.378	155.7	182.7

Figure 10 illustrates the predicted specific impulse from 2D-axisymmetric BLAZE simulations as a function of the nozzle divergence angle for a nozzle geometry having a 0.014" diameter throat, a flow rate of 87 mg/s, and an area ratio of either 51:1, 70:1, or 100:1. There are no dramatic differences in the results, but BLAZE predicts that nozzles with an area ratio of >70:1 should provide a few seconds of I_{sp} advantage, and that a 15° half angle nozzle had the best performance. **Figure 11** illustrates the predicted velocity profiles at the nozzle exit for the 51:1 and 100:1 area ratio 20° conical nozzles. The velocity profiles show a relatively constant exit velocity through most of the nozzle that falls off to zero in the boundary layer region, but also that the 100:1 nozzle has a slightly higher velocity that corresponds with the slightly larger predicted value of Isp shown in **Figure 10**. The fact that the 15° nozzles have the highest I_{sp} is consistent with well-developed nozzle flows in which there is a smaller component of the velocity in the non-thrust directions.

Summary of BLAZE Results

The following summarizes the results from the 2D-axisymmetric BLAZE Multiphysics simulations:

1) Conical nozzles with an area ratio > 70:1 and a divergence half-angle of 15 – 20° are predicted to have the highest thrust and Isp.
2) The contoured and smoothed throat nozzles modeled show no advantage over the conical nozzles.
3) A specific impulse of ~185 seconds should be achievable with CMP-X.

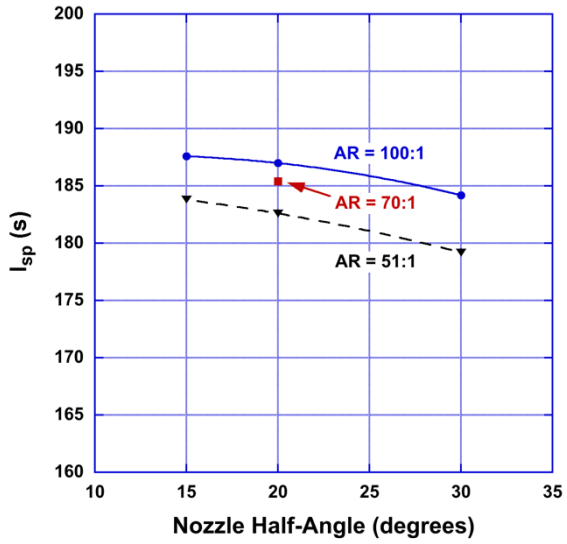

Figure 10. BLAZE predictions of nozzle exit I_{sp} vs. nozzle half-angle as a function of nozzle area ratio. Simulations run for CMP-X with a total temperature of 1223 K and a flow rate of 86.9 mg/s.

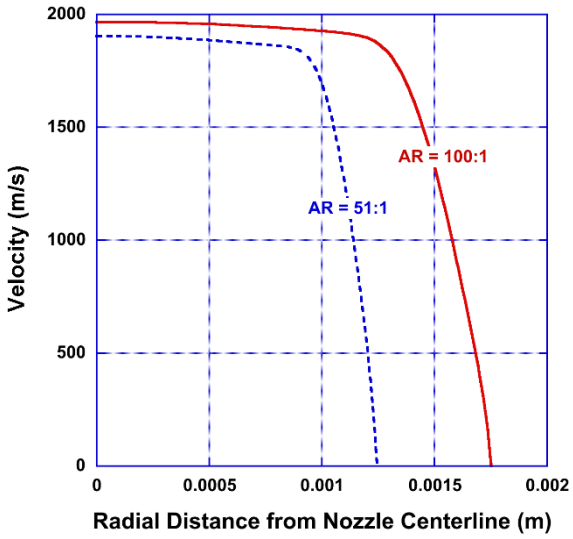

Figure 11. BLAZE predictions for velocity at the nozzle exit plane vs. radial distance from nozzle centerline as a function of area ratio for a 20° half-angle conical nozzle.

THRUST STAND TEST RESULTS

Performance levels at ~90% of theoretical maximum levels have been realized in testing on CUA's compact thrust stand, **Figure 12**. CTF-O3b demonstrated 180 s specific impulse at 174 mN thrust using CMP-X with continuous firing times exceeding 10 minutes that were limited only by feed system volume. **Figures 13** and **14** show the CTF performance as measured on the thrust stand. In all cases shown, the nozzle was a simple cone shape having a 0.014" diameter throat, 20° half-angle, and an exit area ratio of 51, similar to the BLAZE modeling shown earlier. Thrust is approximately linearly proportional to mass flow rate, **Figure 13**, and the specific impulse is shown to increase slightly with mass flow, **Figure 14**. For the data point having 180 s specific impulse at 174 mN thrust, the propellant feed pressure was 179 psia. Note stable operation and sharp transitions between feed rates / thrusts in the raw data presented in **Figure 15**. CUA has burned over 3000 ml of CMP-X in the CTFs to date.

#	Description
1	CUA compact thrust stand
2	electric inlet valve
3	spiral feed system
4	heat wire and thermocouple
5	CTF combustor
6	nozzle
7	pressure drape to feed system
8	~125 mN calibration weights x 4

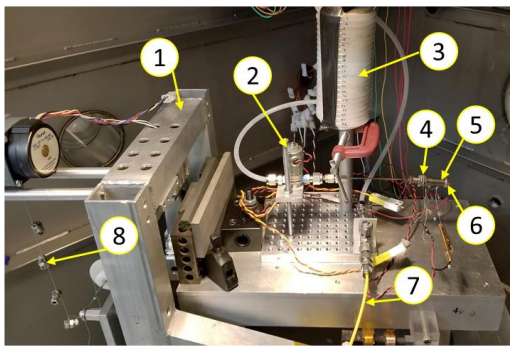

Figure 12. CUA compact thrust stand during CTF testing

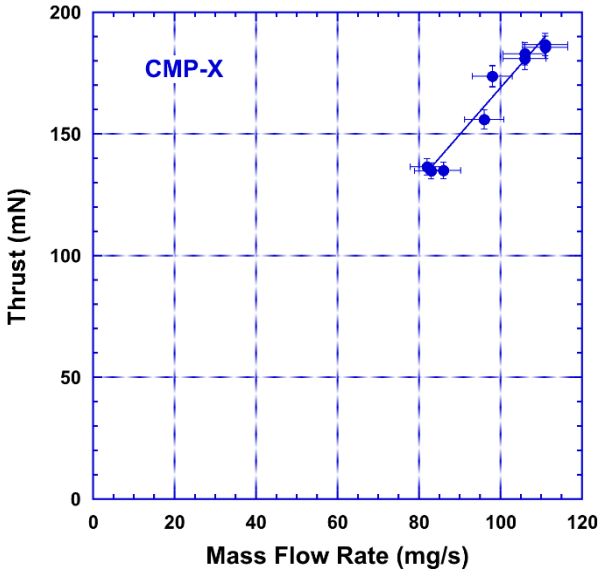

Figure 13: CMP-X thrust versus mass flow rate data taken on CUA's compact thrust stand.

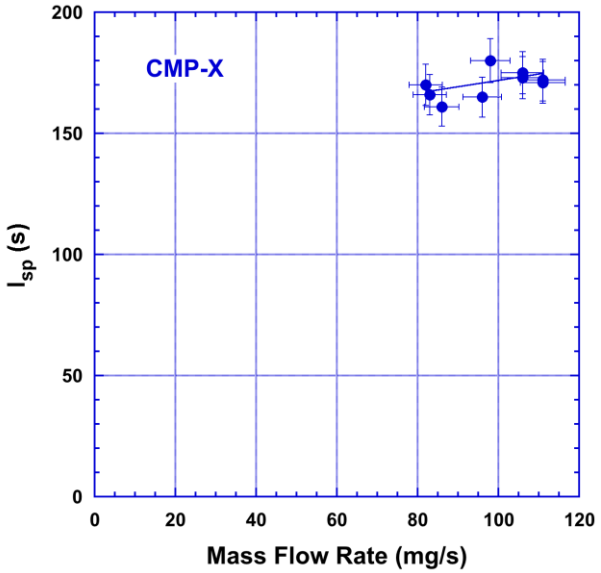

Figure 14: CMP-X I_{sp} versus mass flow rate data taken on CUA's compact thrust stand.

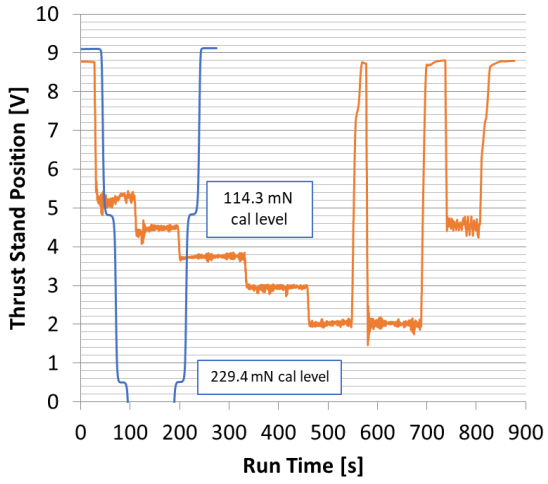

Figure 15. CTF thrust stand raw voltage trace.

To demonstrate the ability to scale the thrust magnitude, an enlarged nozzle throat diameter of 0.027" was fabricated. Available tooling that could be procured rapidly resulted in a larger than desired half-angle of 40°. A limited amount of data was taken as the goal of these tests was just to demonstrate higher thrust rather than focus on optimizing the CTF for this thrust level. Thrust stand measurements, **Figure 15**, demonstrated thrust of 450 mN at 135 psia feed pressure and 521 mN at 155 psia feed pressure (not shown for brevity). The highest Isp measured at the higher thrust levels was 154 s. It is believed that the Isp for these CTF tests was lower than for the lower-thrust series due to: (i) a catalyst bed volume that was too small for the flow rate because it was the same volume as used for the lower-flow series, and (ii) a larger half-angle nozzle was used than desired (note that

extrapolating the BLAZE modeling curves shown in **Figure 10** results in an I_{sp} drop of ~10 s when going from 15° to 40°). With catalyst bed volume optimization, nozzle optimization, and the addition of a radiator, it is strongly believed that the CTF can be made to operate with an Isp of ~180 s at these elevated thrust levels. Regardless, the goal of demonstrating that CMP-X can stably operate at 500 mN was achieved.

A photograph of the CTF-S during operation is shown in **Figure 16**. Thrust stand testing of CTF-S with CMP-X will begin in the near future. Presently, we are optimizing the external temperature measurements from the five-element rake (shown in **Figure 5**). A sample trace is presented as **Figure 17**.

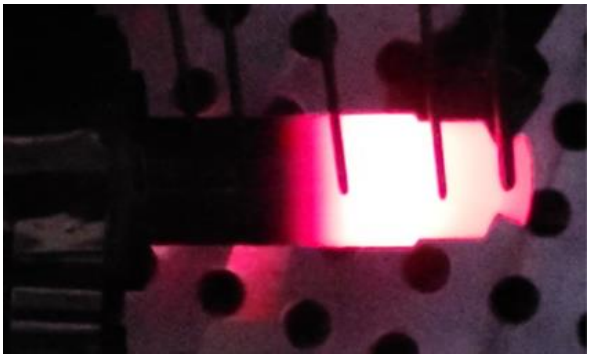

Figure 17. CTF-S during operation (flow is left to right).

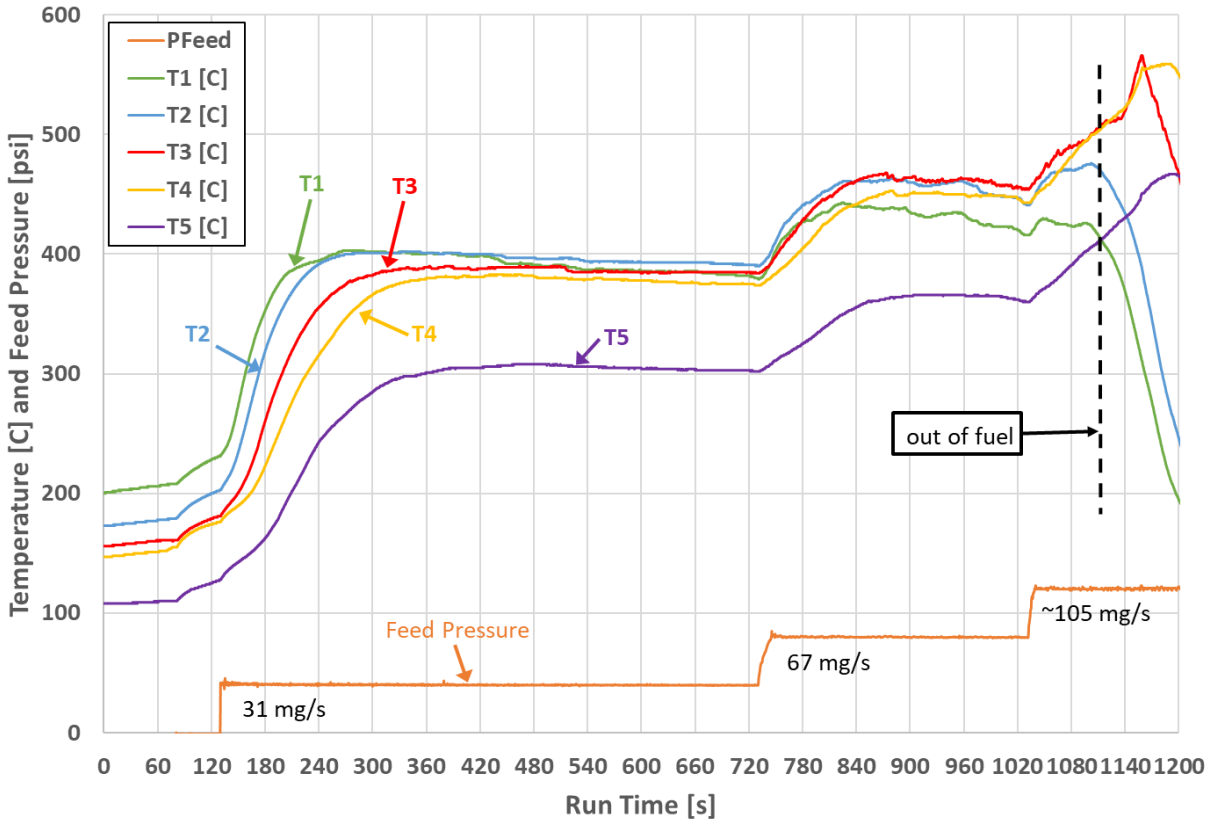

Figure 17. CTF-S experimental thermocouple and pressure feed data.

CONCLUDING REMARKS

CU Aerospace has successfully demonstrated the operation and scalability of its new, low-temperature, intrinsically-safe propellant CMP-X. Specific Impulse is expected near 180 s with thrust levels demonstrated up to 500 mN. Granular iridium-loaded catalyst development was instrumental in extending thruster life at performance levels approaching stoichiometric limits.

Acknowledgments

This work was supported by NASA's SBIR program on contract numbers 80NSSC19C0265 and 80NSSC20C0221 and previously by USAF under SBIR contract FA9300-15-M-1003.

References

1. Spores, R., Masse, R., Kimrel, S., and McLean, C., "GPIM AF-M315E Propulsion System", 49th AIAA/ASME/SAE/ASEE Joint Propulsion Conference & Exhibit, San Jose, CA, July 2013.

2. Tsay, M., Lafko, D., Zwahlen, J., and Costa, W., "Development of Busek 0.5N Green Monopropellant Thruster," 27th Annual AIAA / USU Conference on Small Satellites, SSC13-VII-7, 2013.

3. Masse, R., "AF-M315E Technology Present State-of-the Art, Emerging Capabilities, and Mission Applications", Green Monopropellant Alternatives to Hydrazine JANNAF/NIRPS Joint TIM, August 2015.

4. Tsay, M.; Zwahlen, J.; Lafko, D.; Feng, C.; Robin, M., "Complete EM System Development for Busek's 1U CubeSat Green Propulsion Module," Proc. 52nd AIAA/SAE/ASEE Joint Prop. Conf., AIAA Paper # 2016-4905, 2016.

5. Tsay, M.; Feng, C.; Zwahlen, J., "System-Level Demonstration of Busek's 1U CubeSat Green Propulsion Module 'AMAC'," Proc. 53rd AIAA/SAE/ASEE Joint Propulsion Conf., AIAA Paper # 2017-4946, 2017.

6. Masse, Robert K., Ronald Spores, and May Allen. "AF-M315E Advanced Green Propulsion–GPIM and Beyond." AIAA Propulsion and Energy 2020 Forum. 2020.

7. Dinardi, A. "High Performance Green Propulsion (HPGP)", ECAPS Overview march 2013, [online database].

8. Friedhoff, P.; Hawkins, A.; Carrico, J.; Dyer, J.; Anflo, K., "On-Orbit Operation and Performance of Ammonium Dinitramide (ADN) Based High Performance Green Propulsion (HPGP) Systems," Proc. 53rd AIAA/SAE/ASEE Joint Propulsion Conference, AIAA Paper # 2017-4673, 2017.

9. Wilhelm, M., Negri, M., Ciezki, H., and Schlechtriem, S., "Preliminary tests on thermal ignition of AND-based liquid monopropellants," Acta Astronautica, https://doi.org/10.1016/j.actaastro.2018.05.057 , 2018.

10. Cardin, Joe, Tate Schappell, and Chris Day. "Testing of a Green Monopropellant Integrated Propulsion System." (2020).

11. King, D. M., Woodruff, C., Burton, R. L., and Carroll, D. L., "Development of H2O2-Based Monopropellant Propulsion Unit for CubeSats (MPUC)", JANNAF 2016-4935, Phoenix, AZ, Dec. 2016.

12. Schneider, Steven J. "Hydrogen Peroxide-Water-Ethanol Monopropellant Blend for CubeSat Propulsion." AIAA Propulsion and Energy 2020 Forum. 2020.

13. Hawkins, T.W., Brand, A.F., McKay, M.B., and Tinnirello, M., "Reduced Toxicity, High Performance Monopropellant at the U.S. Air Force Research Laboratory," Air Force Report Number AFRL-RZ-ED-TP-2010-219, 2010.

14. Shanley, E.S. and Perrin, J.R., "Prediction of the Explosive Behavior of Mixtures Containing Hydrogen Peroxide," Jet Propulsion, June 1958.

15. Palla A D, Carroll D L, Verdeyen J T, and Heaven M C, "High-fidelity modelling of an exciplex pumped alkali laser with radiative transport," J. Phys. B: Atomic, Mol. And Opt. Phys., Vol. 44, 135402 (2011).

16. Hejmanowski N J, Woodruff C A, Burton R L, Carroll D L, Palla A D, and Cardin J M (2016), "CubeSat High Impulse Propulsion System (CHIPS) Design and Performance," JANNAF 2016, Paper Tracking # 4800, Phoenix, AZ, Dec. 2016.

17. Woodruff C, Carroll D, King D, Burton R, and Hejmanowski N (2018), "Monofilament Vaporization Propulsion (MVP) – CubeSat propulsion system with inert polymer propellant," Small Satellite Conference, Logan, UT, Paper # SSC18-III-09.